Available online at www.sciencedirect.com
ScienceDirect
Ceramics International 36 (2010) 2169–2174
CERAMICS INTERNATIONAL
www.elsevier.com/locate/ceramint

Monodisperse nanospheres of yttrium oxysulfide: Synthesis, characterization, and luminescent properties

P.F. Ai, W.Y. Li, L.Y. Xiao, Y.D. Li, H.J. Wang, Y.L. Liu *

Department of Chemistry, Jinan University (JNU), 601 Huangpudadaoxi, Tianhe District, Guangzhou, Guangdong 510632, PR China

Received 25 November 2009; received in revised form 29 March 2010; accepted 6 May 2010
Available online 23 June 2010

Abstract

A red long-lasting phosphorescent material, monodisperse Y_2O_2S: Eu^{3+}, Mg^{2+}, Ti^{4+} nanospheres have been prepared successfully. $Y(OH)(CO_3)$: Eu^{3+} nanospheres were firstly synthesized via an urea-based homogeneous precipitation technique to serve as the precursor. Nanospheres long-lasting phosphors Y_2O_2S: Eu^{3+}, Mg^{2+}, Ti^{4+} were obtained by calcinating the precursor in CS_2 atmosphere. XRD investigation shows a pure phase of Y_2O_2S, indicating no other impurity phase appeared. SEM observation reveals that the structures are nanosphere. The Y_2O_2S: Eu^{3+}, Mg^{2+}, Ti^{4+} nanospheres with particle size about 100–150 nm show uniform size and well-dispersed distribution. After irradiation by ultraviolet radiation with 325 nm for 5 min, the phosphor emitted red color long-lasting phosphorescence corresponding to typical emission of Eu^{3+} ion. The main emission peaks are ascribed to Eu^{3+} ions transition from ^5D_J ($J = 0, 1, 2$) to ^7F_J ($J = 0, 1, 2, 3, 4$). Both the PL spectra and luminance decay revealed that this phosphor had efficient luminescent and long-lasting properties. It was considered that the red-emitting long-lasting phosphorescence was due to the persistent energy transfer from the traps to the Ti^{4+} and Mg^{2+} ions.

Keywords: Homogeneous precipitation method; Yttrium oxysulfide; Nanosphere; Luminescence

1. Introduction

With the rapid development of science and technology, the demand for materials is growing rapidly. The particle size of materials should be decreased farther because of the component miniaturization, intelligence, highly integration, high-density storage and ultra-fast transmission [1–4]. During the recent half-century, long-lasting phosphors have been developed rapidly. The afterglow of such phosphors generally lasts for a long time in the darkness and the colors cover from blue to red. Based on the unique property, they have potential applications in many different fields, such as safe indicators, fluorescent lamps, urgent illumination system, cathode ray tubes, etc. [5–9]. Now, Y_2O_2S: Eu^{3+}, Mg^{2+}, Ti^{4+} micron-phosphor is unable to meet the needs of society. Therefore, the preparation of Y_2O_2S: Eu^{3+}, Mg^{2+}, Ti^{4+} nano-phosphor are great significant in the optical material research.

Nowadays, the development of the long-lasting phosphors focus on the materials which with nanostructures [10–13]. After ultra-fine or nanometer treatment, Y_2O_2S: Eu^{3+}, Mg^{2+}, Ti^{4+} phosphorescent material shows a lot of new optical, electrical characters and has an unmatchable advantage in comparison with the bulk materials [14–16], because of the nano-effects which include size effect, surface state effects, etc.

Until now, there is still no conclusion on the impact about the nano-effect on the luminescence properties of rare earth compounds and luminescent materials, the research results obtained are quite different and even sometimes on opposite [17]. In addition, the difference between nano-materials preparation technologies can also cause many factors which affect on the powders of different morphology, particle size distribution and luminescence properties. So there much work about the properties of nano-rare earth luminescent materials should be done.

At present, this kind of nano-powder phosphor is synthesized generally by wet-chemical method [4,18]. Scientists have made prominent contribution in the relevant fields. La_2O_2S ultra-fine powder materials were synthesized by anhydrous ethanol as a solvent system through solvothermal

* Corresponding author. Tel.: +86 20 85221813; fax: +86 20 85221697.
E-mail address: tliuyl@jnu.edu.cn (Y.L. Liu).

0272-8842/$36.00.
doi:10.1016/j.ceramint.2010.05.025

under 300 °C [19]. However, a series of nano-rare earth oxysulfides including La_2O_2S, Eu_2O_2S, etc. were synthesized by solvothermal under 150 °C. To further reduce the reaction temperature, they used the ethylenediamine as a solvent system. Whereas, the failure on the synthesis of Y_2O_2S: Eu^{3+}, Mg^{2+}, Ti^{4+} nano-powder can be ascribed to the lower temperature in the process of the solvothermal [20]. Micron-powders were synthesized by increasing the temperature to 280 °C in the process of solvothermal [21]. Therefore, how to make Y_2O_2S: Eu^{3+}, Mg^{2+}, Ti^{4+} nano-long afterglow phosphor is still a challenging job.

In this paper, we propose an effective method to prepare nanosphere red long-lasting phosphors with uniform size and well-dispersed distribution. Y_2O_2S: Eu^{3+}, Mg^{2+}, Ti^{4+} nanospheres have been prepared by using urea as the precipitant through homogeneous precipitation technique followed by sulfur treatment process in CS_2 atmosphere [22]. The homogeneous precipitation technique which exhibits some advantages of low processing temperature, high homogeneity and purity of the products has become a promising method for the preparation of nanospherical materials. Such well-dispersed Y_2O_2S: Eu^{3+}, Mg^{2+}, Ti^{4+} nanospheres show persistent red emission after UV illumination at room temperature, exhibiting potential in photoluminescent application. The results indicate that the nanosphere Y_2O_2S: Eu^{3+}, Mg^{2+}, Ti^{4+} phosphor has promising long-lasting phosphorescence in potential applications with good thermal stability, high chemical durability and low cost.

2. Experimental

The experiment consisted of two steps. Firstly, 0.1 mol Y_2O_3, 0.008 mol Eu_2O_3 was dissolved in concentrated HNO_3. Then appropriate amount of urea was added into $Y(NO_3)_3$ and $Eu(NO_3)_3$ aqueous solution with vigorous stirring for 2 h to form a clear solution, kept the concentration of urea 0.5 mol l^{-1}. And then mixture began to react when the mixture was heated to 90 °C. When the production was cooled down to about 50 °C naturally after reacting completely, white $Y(OH)(CO_3)$: Eu^{3+} precipitations were collected. The co-precipitated precursors were filtered, washed with distilled water and ethanol three times each, and finally dried at 100 °C for 24 h.

In the second step, Y_2O_2S: Eu^{3+}, Mg^{2+}, Ti^{4+} phosphors were prepared by a gas aided sulfur treatment through calcining $Y(OH)(CO_3)$: Eu^{3+} precursor using CS_2 as a sulfurization agent. Sulfur powder was put in a sealed graphite crucible, and pre-fired at 800 °C for 4 h. During the heat treatment, sulfur reacted with graphite to form CS_2, which was absorbed in the vacancies within the graphite layer. Then the dried precursors together with the mixture of 0.001 mol $Mg(OH)_2{\bullet}4Mg$-$4MgCO_3{\bullet}6H_2O$, 0.001 mol TiO_2 were placed into the graphite crucible and calcined at 1100 °C for 4 h.

Both the as-prepared $Y(OH)(CO_3)$: Eu^{3+} precursor and the final Y_2O_2S: Eu^{3+}, Mg^{2+}, Ti^{4+} phosphorescent products were characterized. The structures of the products were determined by a Rigaku Model D/max-II B X-ray diffractometer with Cu $K\alpha_1$ ($\lambda = 0.15405$ nm) radiation at a 0.02° (2θ) min^{-1} scanning step. The morphologies of the powder were observed by employing scanning electron microscopy (SEM, Philips XL-30) and transmission electron microscopy (TEM, Philips TECNAI 10), the photoluminescence spectra and intensity were measured by a spectra fluorophotometer (Hitachi F-4500). The thermoluminescence (TL) spectra were measured by FJ427A1 (China) in the temperature range of 30–300 °C at a heating rate of 2 °C/s. All measurements were carried out at room temperature expect for the TL spectra.

3. Results and discussion

3.1. Crystal structure of the products

To make sure our results are reliable, we prepared our samples and checked their structures carefully. Fig. 1 shows the XRD patterns of the precursor generated by homogeneous precipitation technique and Y_2O_2S: Eu^{3+}, Mg^{2+}, Ti^{4+} powders after being calcined at different temperatures. No obvious diffraction peak appears in Fig. 1a, which indicates that the precursor compound is amorphous without calcination. It is obvious from Fig. 1b that the sample calcinated under 1000 °C has a cubic Y_2O_3 structure, while the other two samples (Fig. 1c and d) possess hexagonal Y_2O_2S structure. For the product calcined at 1100 °C for 4 h, the XRD patterns of the powder match well with the values in the standard Y_2O_2S card (JCPDS No.24-1424). The phase analysis demonstrates that Y_2O_2S: Eu^{3+}, Mg^{2+}, Ti^{4+} has hexagonal crystal structure with the unit cell dimensions: $a = 0.385$ nm, $c = 0.666$ nm, which are very close to the standard lattice parameters provided by the powder diffraction file, PDF #24-1424. Obviously, the substitution of Y^{3+} with trace Eu^{3+}, Mg^{2+} and Ti^{4+} does not remarkably change the crystal structure and lattice parameters of Y_2O_2S.

3.2. Morphology of the $Y(OH)(CO_3)$: Eu^{3+} precursor

The microstructures of $Y(OH)(CO_3)$: Eu^{3+} precursor are studied by the SEM patterns and presented in Fig. 2. It can be

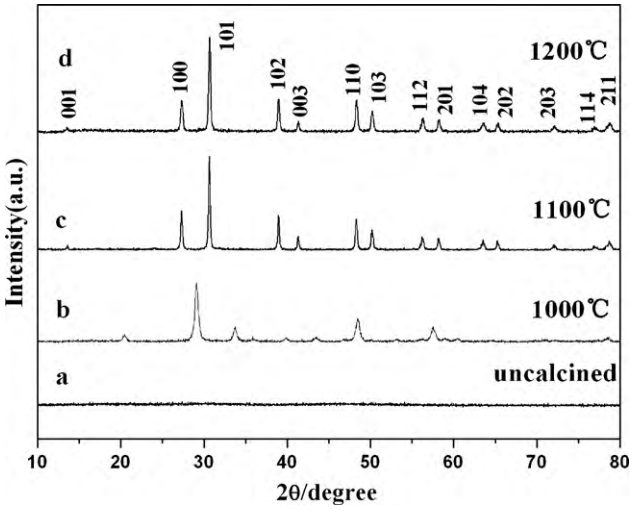

Fig. 1. XRD patterns of (a) the precursor generated by homogeneous precipitation technique and Y_2O_2S: Eu^{3+}, Mg^{2+}, Ti^{4+} powders after being calcined at (b) 1000 °C; (c) 1100 °C; and (d) 1200 °C.

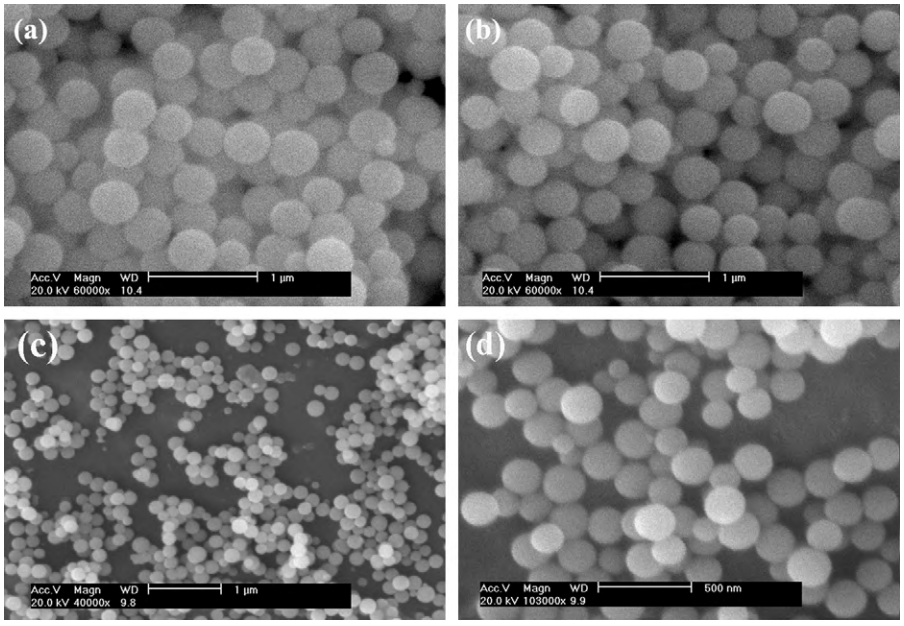

Fig. 2. The SEM images of the $Y(OH)(CO_3)$: Eu^{3+} precursor with the different in the concentration of Eu^{3+}-doped (a) 4%; (b) 6%; (c) and (d) 8%.

seen from the micrograph that the sample possesses a large number of uniform nanospheres. With the increase in the concentration of Eu^{3+}-doped (4%, 6%, 8%), nanospheres can be obtained with the diameter reduced from 400–500 nm to 80–150 nm gradually. Large number of studies show that the nanospheres with lesser particle size and better dispersion can be obtained by increasing the concentration of Eu^{3+}-doped. It could be concluded from the figures that a suitable Eu^{3+} concentration in precursor is around at 8%, and the nanospheres with the diameter of 80–150 nm (Fig. 2c and d).

3.3. Morphology of the Y_2O_2S: Eu^{3+}, Mg^{2+}, Ti^{4+} nanospheres

Morphology of the sulfur treatment synthesized Y_2O_2S: Eu^{3+}, Mg^{2+}, Ti^{4+} is investigated by SEM, as followed in Fig. 3. The calcination of the precursor in CS_2 atmosphere leads to the formation of Y_2O_2S: Eu^{3+}, Mg^{2+}, Ti^{4+}. It also can be seen that the sizes of these oxysulfide nanospheres are similar to the initial precursor, implying that the shape of nanospheres can be still kept even through the high-temperature sulfur treatment process. The shape of nanosphere precursor can be inherited to Y_2O_2S only by calcination in CS_2 environment.

It should also be noted here that a suitable calcinating temperature is required for the preparation of pure phased Y_2O_2S: Eu^{3+}, Mg^{2+}, Ti^{4+} nanosphere. When sulfured at 1000 °C (Fig. 3a), the Y_2O_3 monodisperse nanosphere which inherit the shape of precursor completely with size of 100–200 nm can be obtained. When the temperature of sulfur is 1100 °C (Fig. 3b and c), pure phased Y_2O_2S: Eu^{3+}, Mg^{2+}, Ti^{4+} can be obtained. All the structure shows nanosphere shape with diameter of 100–150 nm and well-dispersed can also be observed. When the temperature rises to 1200 °C (Fig. 3d), some particles are agglomerate and the morphology of nanoparticles has been subverted into irregularly shaped particles because the temperature of sulfur is too high. Therefore, the suitable temperature for the preparation of nanosphere Y_2O_2S: Eu^{3+}, Mg^{2+}, Ti^{4+} is around 1100 °C.

Compared with our previous experiments [23], it is found that the final products could not remain the shape of precursor by using other flowing gas but not CS_2. Preliminarily, we can conclude that the atmosphere, in which the precursor is calcined, plays an important role in keeping the shape of the nanosphere. Additionally, this atmosphere may be a key factor for a close morphological retention between the precursor and the final products nanosphere Y_2O_2S. Therefore, we also need an elaborate research on the mechanism to explain the details about this process.

3.4. Luminescence property of the red phosphor

Fig. 4 illustrates the excitation and emission spectra of nanosphere Y_2O_2S: Eu^{3+}, Mg^{2+}, Ti^{4+} phosphors calcined in CS_2 atmosphere under 1100 °C for 4 h. It is clear that the emission spectra and the excitation spectra are similar to bulk Y_2O_2S: Eu^{3+}, Mg^{2+}, Ti^{4+} phosphor. It is clear from Fig. 4a that the excitation spectrum is a wide band with two peaks attributing to the Eu^{3+}–O^{2-} CTB (charge transfer band) and Eu^{3+}–S^{2-} CTB. For bulk Y_2O_2S: Eu^{3+}, Mg^{2+}, Ti^{4+}, one at 266 nm corresponds to Eu^{3+}-O^{2-} CTB, and the other at 315 nm to Eu^{3+}–S^{2-} CTB. For nanosphere Y_2O_2S: Eu^{3+}, Mg^{2+}, Ti^{4+}; One at 260 nm corresponds to Eu^{3+}–O^{2-} CTB, and the other at 325 nm corresponds to Eu^{3+}–S^{2-} CTB. The emission spectra of bulk and nanosphere Y_2O_2S: Eu^{3+}, Mg^{2+}, Ti^{4+} phosphors were shown in Fig. 4b. When the phosphors are excited by 325 nm, they produce visible light with different wavelengths. This indicates the typical intrinsic transition of Eu^{3+} within different energy levels. The strongest red-emission line at 615 and

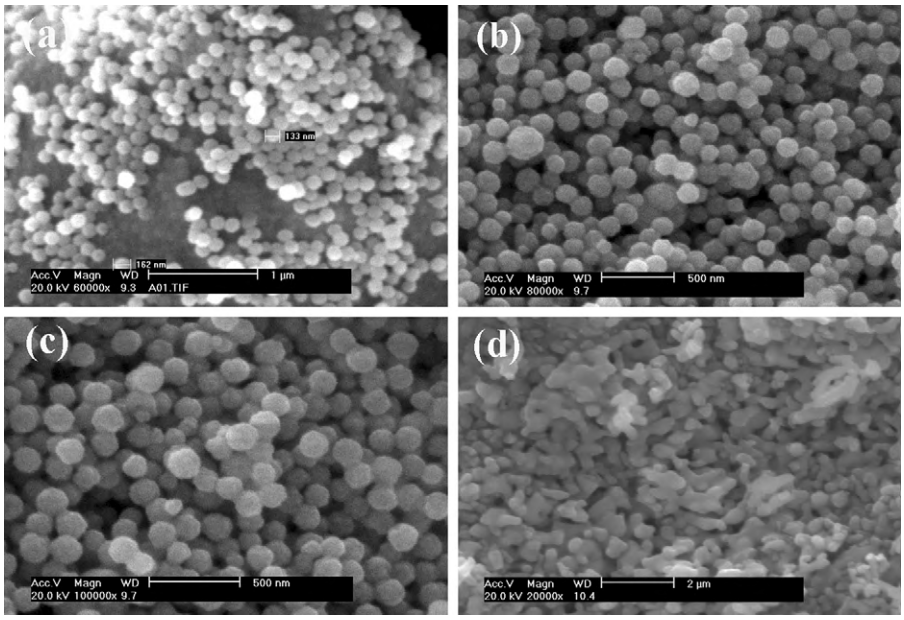

Fig. 3. The SEM images of the sulfur treatment synthesized Y_2O_2S: Eu^{3+}, Mg^{2+}, Ti^{4+} at (a) 1000 °C; (b) and (c) 1100 °C; and (d) 1200 °C.

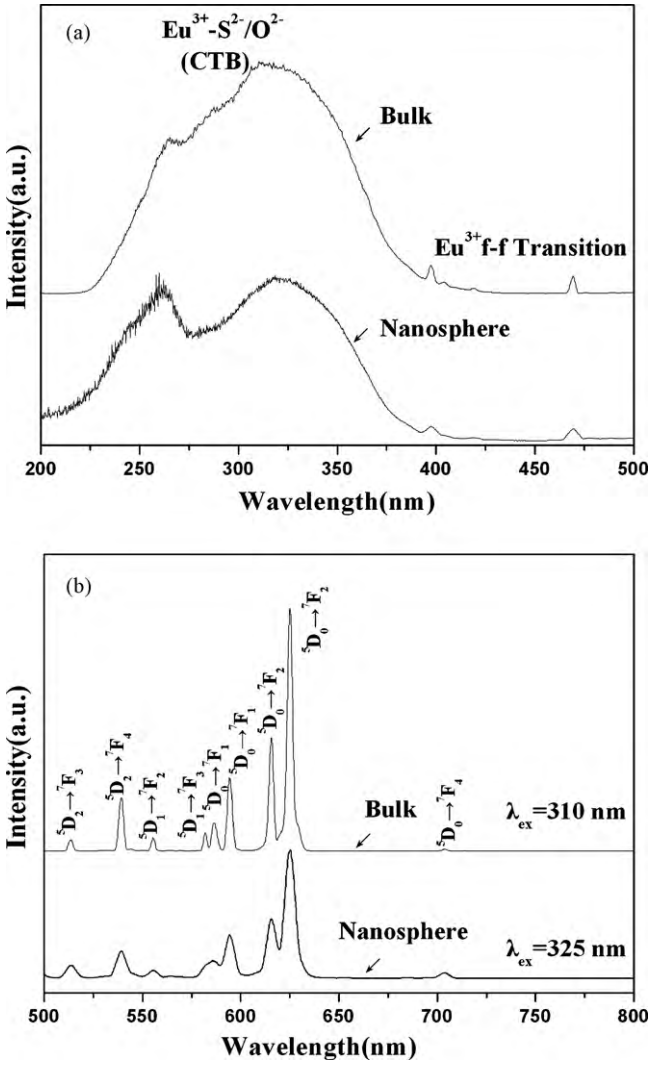

Fig. 4. (a) Excitation and (b) emission spectra of the Y_2O_2S: Eu^{3+}, Mg^{2+}, Ti^{4+} phosphors.

625 nm corresponds to transition from $^5D_0$ to $^7F_2$ level of Eu^{3+} ion. From the emission spectra, we can confirm the formation of the oxysulfide host by the strongest emission at λ_{em} = 625 nm. Nonetheless, either Mg^{2+} or Ti^{4+} ion does not change the shape of excitation and emission spectra dramatically. Compared with bulk material, the excitation bands in nanosphere show no apparent blue-shift.

3.5. Afterglow decay curves of the red phosphors

The afterglow decay curve of the nanosphere Y_2O_2S: Eu^{3+}, Mg^{2+}, Ti^{4+} phosphor calcined under 1100 °C is shown in Fig. 5. It is obvious that co-doped Mg^{2+} and Ti^{4+} ions can lead to long afterglow. The phosphor shows a rapid decay at the beginning and the long-lasting phosphorescence further. The afterglow mechanisms can be explained by the contribution from the electron traps formed by the co-doped Mg^{2+} and Ti^{4+} ions.

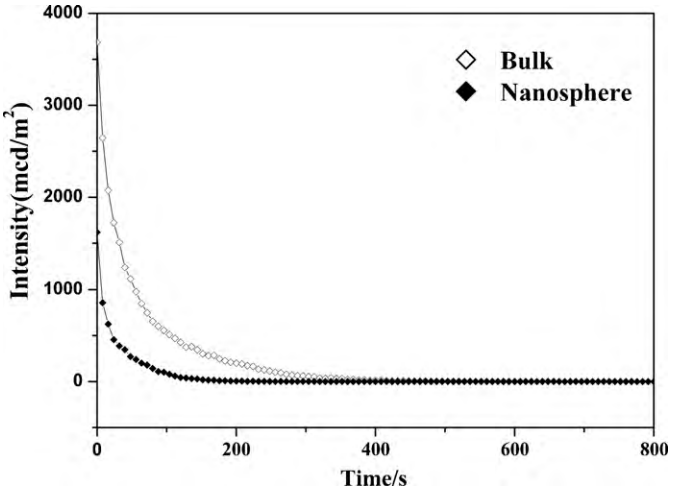

Fig. 5. The decay curve of the Y_2O_2S: Eu^{3+}, Mg^{2+}, Ti^{4+} phosphors.

When the Y_2O_2S: Eu^{3+} phosphor is co-doped with both Mg^{2+} and Ti^{4+}, the Mg^{2+} and Ti^{4+} ions occupy the same lattice sites as Y^{3+} ions do. To keep charge balance, 2 Y^{3+} ions were replaced by 1 Ti^{4+} and 1 Mg^{2+} ion. However, such replacement breaks the charge balance around local lattice site and causes the formation of new electronic donating and accepting levels between the host lattice band gap, that is, an excessive positive charge which serves as the electron trap around the doped Ti^{4+} ion was created. One of ions absorbs energy and thermally transfers the excited electrons to another ion which serves as trap centers. The trap of stored energy which is constituted by Ti^{4+} and Mg^{2+} ions serves as the donor leveling, and Eu^{3+} serves as the acceptor leveling. The trapping of excited electrons and thermally released processes cause the appearance of afterglow [7,22].

It is clear that the afterglow decay curves are different between nanosphere Y_2O_2S: Eu^{3+}, Mg^{2+}, Ti^{4+} phosphors and bulk sample. After ultra-fine or nanometer treatment of phosphorescent material, the afterglow property will be reduced because of the decrease of particle size, the increase of specific surface area and the surface defects. Therefore, the afterglow property of phosphorescent material with smaller particle size is not as well as bulk material.

3.6. Thermoluminescence for the red phosphor

From the reports [24], the glow peaks between 323 and 383 K in the thermo-luminescent curve benefit the appearance of afterglow. It is obvious that there is a peak around 360 K, which is related to the afterglow of Y_2O_2S: Eu^{3+}, Mg^{2+}, Ti^{4+} phosphor. As is shown in Fig. 6, thermo-luminescent curve of nanosphere Y_2O_2S: Eu^{3+}, Mg^{2+}, Ti^{4+} phosphor is similar to the bulk sample. According to the report [25], the defects introduced by doped ions played a key role in the long-lasting phenomenon. The doped Mg^{2+} and Ti^{4+} ions may replace Y^{3+} to shape some defects to capture free electrons and holes. During the heat process, the holes or electrons trapped will be released, and then the electron–hole recombination produces afterglow phenomenon. The trap energy level can be estimated using the following half peak width method [26]:

$$E = \frac{2k(T_m)^2}{T_2 - T_m} \quad (1)$$

where k is the Boltzmann's constant; T_m the temperature value corresponding to the peak of the thermo-luminescent curve; T_2 the temperature value corresponding to the point on the right side of the thermo-luminescent curve, where the peak intensity is half of the peak value. By calculating the traps energy level of the nanosphere Y_2O_2S: Eu^{3+}, Mg^{2+}, Ti^{4+} phosphor is about 0.52 eV, which shows a suitable trap depth and therefore produces long-lasting afterglow for the nanosphere Y_2O_2S: Eu^{3+}, Mg^{2+}, Ti^{4+} phosphor.

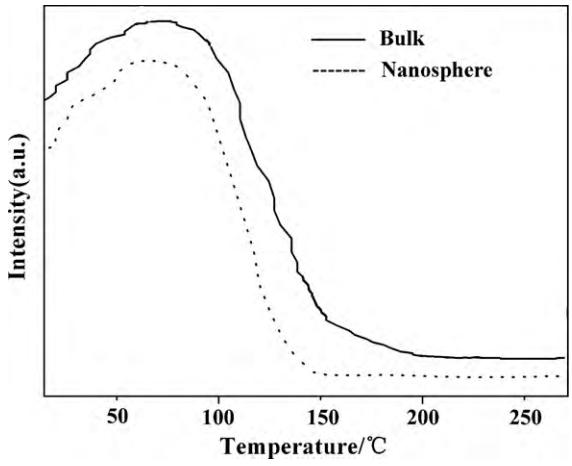

Fig. 6. The thermo-luminescent curve of the Y_2O_2S: Eu^{3+}, Mg^{2+}, Ti^{4+} phosphors.

4. Conclusion

In this paper, a promising red long-lasting phosphorescent material, single crystalline nanospheres Y_2O_2S: Eu^{3+}, Mg^{2+}, Ti^{4+}, has been prepared through urea-based homogeneous precipitation technique followed by a subsequent sulfur treatment process. The results show that the final product with smooth surface and uniform size of 100–150 nm inherited the nanosphere structure from the precursor calcined in CS_2 atmosphere at 1100 °C for 4 h. When excited by 325 nm, the phosphor has a very strong and broad emission band at 625 nm, which is attributed to the transition of Eu^{3+} between the $^5D_0$ states and $^7F_2$ states. The introduction of Mg^{2+} and Ti^{4+} ions is good for the formation of complex holes and electron traps, which result in the long-lasting phenomenon.

Acknowledgments

This present work was financially supported by the National Natural Science Foundations of China (Nos. 20671042 and 50872045) and the Natural Science Foundations of Guangdong Province (Nos. 05200555 and 7005918).

References

[1] X.F. Duan, C.M. Lieber, General synthesis of compound semiconductor nanowires, Adv. Mater. 12 (2000) 298–302.
[2] B. Wiley, Y.G. Sun, B. Mayers, Y.N. Xia, Shape-controlled synthesis of metal nanostructures: the case of silver, Chem. Eur. J. 11 (2005) 454–463.
[3] D.W. Wang, Y.L. Chang, Q. Wang, J. Cao, D.B. Farmer, R.G. Gordon, H.J. Dai, Surface chemistry and electrical properties of germanium nanowires, J. Am. Chem. Soc. 126 (2004) 11602–11611.
[4] M. Yada, M. Mihara, S. Mouri, M. Kuroki, T. Kijima, Rare earth (Er, Tm, Yb, Lu) oxide nanotubes templated by dodecylsulfate assemblies, Adv. Mater. 14 (2002) 309–313.
[5] Y.H. Lin, Z.L. Tang, Z.T. Zhang, Anomalous luminescence in $Sr_4Al_{14}O_{25}$: Eu, Dy phosphors, Appl. Phys. Lett. 81 (2002) 996–998.
[6] D. Jia, X. Wang, W. Jia, W.M. Yen, Persistent energy transfer in $CaAl_2O_4$: Tb^{3+}, Ce^{3+}, J. Appl. Phys. 93 (2003) 148–152.
[7] H.H. Zeng, X.M. Zhou, L. Zhang, X.P. Dong, Synthesis and luminescence properties of a novel red long lasting phosphor Y_2O_2S: Eu^{3+}, Si^{4+}, Zn^{2+}, J. Alloys Compd. 460 (2008) 704–707.

[8] M. Kamada, J. Murakami, N. Ohno, Excitation spectra of a long-persistent phosphor $SrAl_2O_4$: Eu, Dy in vacuum ultraviolet region, J. Lumin. 87–89 (2000) 1042–1044.
[9] X.X. Wang, Z.T. Zhang, Z.L. Tang, Y.H. Lin, Characterization and properties of a red and orange Y_2O_2S-based long afterglow phosphor, Mater. Chem. Phys. 80 (2003) 1–5.
[10] W.Y. Li, Y.L. Liu, P.F. Ai, Synthesis and luminescence properties of red long-lasting phosphor Y_2O_2S: Eu^{3+}, Mg^{2+}, Ti^{4+} nanoparticles, Mater. Chem. Phys. 119 (1–2) (2010) 52–56.
[11] Y. Jiang, Y. Wu, Y. Xie, Y.T. Qian, Synthesis and characterization of nanocrystalline lanthanide oxysulfide via a $La(OH)_3$ gel solvothermal route, J. Am. Ceram. Soc. 83 (10) (2000) 2628–2630.
[12] Y.B. Mao, J.Y. Huang, R. Ostroumov, K.L. Wang, J.P. Chang, Synthesis and luminescence properties of erbium-doped Y_2O_3 nanotubes, J. Phys. Chem. C 112 (2008) 2278–2285.
[13] F. Zhao, M. Yuan, W. Zhang, S. Gao, Monodisperse lanthanide oxysulfide nanocrystals, J. Am. Chem. Soc. 128 (2006) 11758–11759.
[14] Y.L. Liu, C.Y. Song, J.X. Zhang, D.S. Yuan, L.H. Huang, J.W. Zhang, Afterglow emission of Er^{3+}, Ho^{3+} and Tm^{3+} in gadolinium oxysulfide, Chin. J. Inorg. Chem. 21 (2005) 905–909.
[15] J.W. Zhang, Y.L. Liu, S.Q. Man, Afterglow phenomenon in erbium and titanium codoped GD_2O_2S phosphors, J. Lumin. 117 (2006) 141–146.
[16] B.F. Lei, Y.L. Liu, G.B. Tang, Z.R. Ye, C.S. Shi, Spectra and long-lasting properties of Sm^{3+}-doped yttrium oxysulfide phosphor, Mater. Chem. Phys. 87 (1) (2004) 227–232.
[17] Q. Li, L. Gao, D.S. Yan, Recent advances in nanoscale luminescent materials of rare earth compounds, J. Inorg. Mater. 16 (1) (2001) 17–22.
[18] G.S. Wu, L.D. Zhang, B.C. Cheng, T. Xie, X.Y. Yuan, Synthesis of Eu_2O_3 nanotubes arrays through a facile sol-gel template approach, J. Am. Chem. Soc. 19 (2004) 5976–5977.
[19] S.H. Yu, Z.H. Han, J. Yang, H.Q. Zhao, R.Y. Yang, Y. Xie, Y.T. Qian, Y.H. Zhang, Synthesis and formation mechanism of La_2O_2S via a novel solvothermal pressure-relief process, Chem. Mater. 11 (2) (1999) 192–194.
[20] Y.D. Li, Y. Huang, T. Bai, L.Q. Li, Straightforward conversion route to nanocrystalline monothiooxides of rare earths through a high-temperature colloid technique, Inorg. Chem. 39 (15) (2000) 3418–3420.
[21] J.Y. Kuang, Y.L. Liu, D.S. Yuan, Preparation and characterization of Y_2O_2S: Eu^{3+} phosphor via one-step solvothermal process, Electrochem. Solid-State Lett. 8 (9) (2005) H72–H74.
[22] S.P. Mao, Q. Liu, M. Gu, D.L. Mao, C.K. Chang, Long lasting phosphorescence of Gd_2O_2S: Eu, Ti, Mg nanorods via a hydrothermal routine, J. Alloys Compd. 465 (2008) 367–374.
[23] W.Y. Li, Y.L. Liu, P.F. Ai, Synthesis of nanocrystalline Y_2O_2S: Eu^{3+}, Mg, Ti long-lasting phosphorescent materials by hydrothermal-microwave method, Chin. J. Inorg. Chem. 24 (2008) 772–776.
[24] M. Ihara, T. Igarashi, T. Kusunoki, K. Ohno, Cathodoluminescence and photoluminescence of nanocrystal phosphors, J. Electrochem. Soc. 149 (2002) H72–H75.
[25] J. Qiu, A.L. Gaeta, K. Hirao, Long-lasting phosphorescence in oxygen-deficient Ge-doped silica glasses at room temperature, Chem. Phys. Lett. 333 (2001) 236–241.
[26] J. Geng, Z.P. Wu, W. Chen, L. Luo, Properties of long afterglow $SrAl_2O_4$: Eu^{2+}, Dy^{3+} phosphor, J. Inorg. Mater. 175 (2) (2003) 480–484.